nature biotechnology

Systemic administration of optimized aptamer-siRNA chimeras promotes regression of PSMA-expressing tumors

Justin P Dassie[1,2,5], Xiu-ying Liu[1,5], Gregory S Thomas[1,2,5], Ryan M Whitaker[1], Kristina W Thiel[1], Katie R Stockdale[1], David K Meyerholz[3], Anton P McCaffrey[1,2], James O McNamara II[1] & Paloma H Giangrande[1,2,4]

Prostate cancer cells expressing prostate-specific membrane antigen (PSMA) have been targeted with RNA aptamer–small interfering (si)RNA chimeras, but therapeutic efficacy *in vivo* was demonstrated only with intratumoral injection. Clinical translation of this approach will require chimeras that are effective when administered systemically and are amenable to chemical synthesis. To these ends, we enhanced the silencing activity and specificity of aptamer-siRNA chimeras by incorporating modifications that enable more efficient processing of the siRNA by the cellular machinery. These included adding 2-nucleotide 3′-overhangs and optimizing the thermodynamic profile and structure of the duplex to favor processing of the siRNA guide strand. We also truncated the aptamer portion of the chimeras to facilitate large-scale chemical synthesis. The optimized chimeras resulted in pronounced regression of PSMA-expressing tumors in athymic mice after systemic administration. Anti-tumor activity was further enhanced by appending a polyethylene glycol moiety, which increased the chimeras' circulating half-life.

Treatment of advanced prostate cancer relies mainly on nonspecific therapies, such as chemotherapies and ionizing radiation, which have low efficacy and are highly toxic to normal tissues[1,2]. Gene-specific mRNA knockdown with synthetic siRNAs may offer several advantages over these approaches[3–5], including target specificity, ease of siRNA production and the possibility of silencing virtually any gene. In addition, recent advances in the understanding of the molecular mechanisms of RNA interference (RNAi) enable rational optimization of the potency, specificity and *in vivo* activity of siRNAs[6–10]. However, before siRNAs can be broadly used in the clinic, safe and effective approaches for their targeted delivery *in vivo* must be developed[11].

Most siRNA targeting approaches involve the formation of siRNA-containing complexes that also include charged peptides[12,13], proteins[14,15] or polymers[16–20]. Although these reagents silence the targeted genes when administered systemically in experimental animals, their complicated formulation is likely to confound their large-scale production and regulatory approval. The potential toxicity of the materials used poses another challenge. As a result, applications involving the direct local delivery (for example, to the eye and lung) of naked or nuclease-resistant (chemically modified) siRNA duplexes have been the first to be evaluated in clinical trials[10,21–24].

We previously developed a simple RNA-only approach for delivering cytotoxic siRNAs targeting prostate cancer–specific pro-survival genes (*Plk1* and *Bcl2*) directly to prostate cancer cells via an RNA aptamer[25]. The aptamer portion of these chimeras binds PSMA[25,26], undergoes cell internalization and delivers its siRNA cargo to the intracellular RNAi machinery. This results in the silencing of the siRNA target gene and pronounced cancer cell death *in vitro*. When injected intratumorally, the PSMA-targeting chimera substantially decreased tumor volume in a xenograft mouse model of prostate cancer[25], inducing apoptosis only in tumors expressing PSMA and having no adverse effects on PSMA-negative tumors or normal cells. Although the first-generation PSMA-binding aptamer/Plk1-siRNA (A10-Plk1) chimera inhibited tumor growth when administered intratumorally[25], systemic administration will be necessary for treatment of advanced prostate cancer, thus presenting a variety of additional challenges. In particular, systemic administration requires greater therapeutic doses (leading to higher treatment costs), and carries a greater risk for harmful side effects owing to greater therapeutic exposure of nontargeted tissues. Improvements that would minimize the necessary dose of the chimera would reduce both the cost of treatment and the risk for harmful side effects. Toward this end, we have modified several aspects of the A10-Plk1chimera. The resulting optimized chimeras exhibit potent antitumor activity when administered systemically to mice bearing PSMA-positive prostate cancer tumors.

RESULTS

Second-generation optimized PSMA-Plk1 chimeras

We designed second-generation PSMA-Plk1 chimeras, aiming to (i) facilitate chemical synthesis, (ii) enhance silencing activity and specificity and (iii) enable modifications to optimize *in vivo* kinetics. Representative second-generation PSMA-Plk1 chimeras developed in this study are shown in **Figure 1**.

To facilitate chemical synthesis, we reduced the aptamer portion of the A10-Plk1chimera from 71 (corresponding to original A10 aptamer)[26] to 39 nucleotides (nt) (A10-3.2 aptamer)). The longer RNA

[1]Department of Internal Medicine, [2]Molecular and Cellular Biology Program, [3]Department of Pathology and [4]Department of Radiation Oncology, University of Iowa, Iowa City, Iowa, USA. [5]These authors contributed equally to this work. Correspondence should be addressed to P.H.G. (paloma-giangrande@uiowa.edu).

Received 23 June; accepted 31 July; published online 23 August 2009; doi:10.1038/nbt.1560

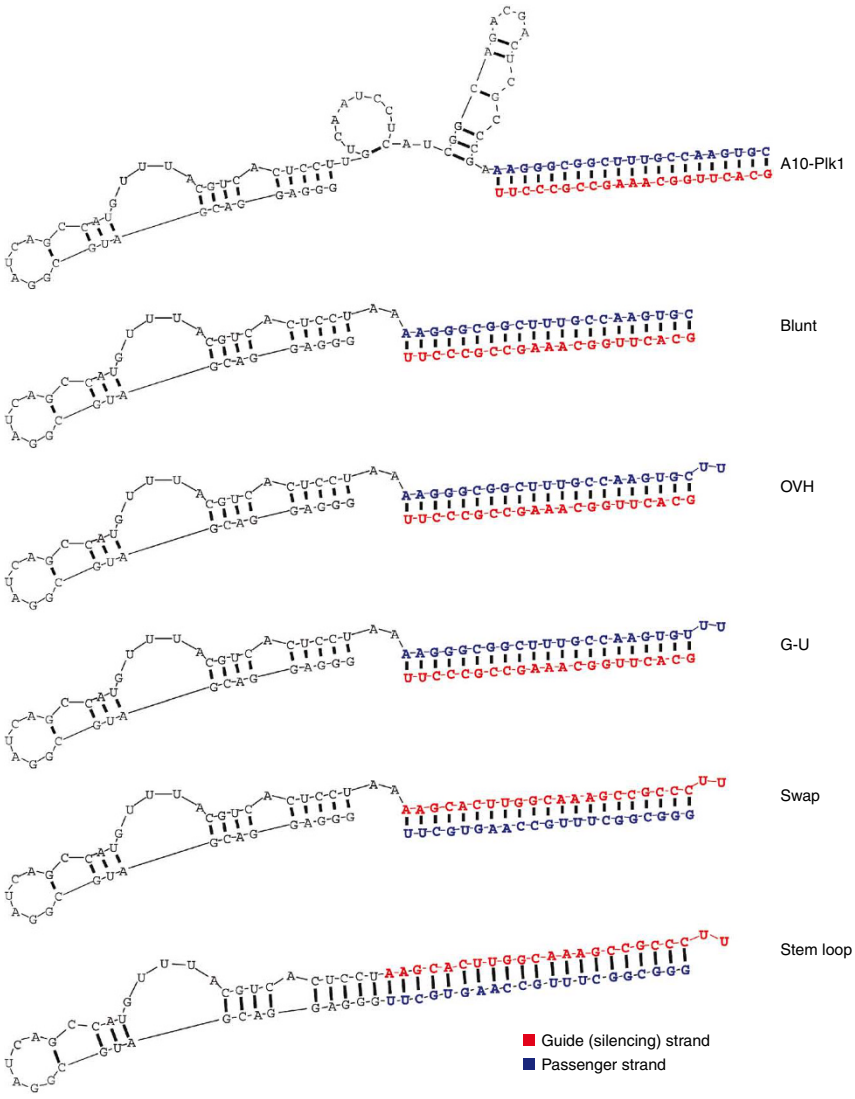

Figure 1 Optimized PSMA-Plk1 chimeras. Blunt, truncated version of first-generation chimera (A10-Plk1) described previously[25]. The aptamer portion of the chimera has been truncated from 71+ nt to 39 nt. OVH, overhang chimera similar to blunt, but with 2 nt (UU)-overhangs at the 3′ end of the siRNA duplex. G-U, G-U wobble chimera identical to OVH, but with a wobble base pair at the 5′ end of the antisense siRNA strand (silencing/guide strand). Swap, sense and antisense strands of siRNA duplex are reversed. Stem loop, hairpin chimera where the siRNA duplex (stem) is continuous with the aptamer (loop). Structural predictions were generated using RNAstructure V 4.6.

strand of the second-generation chimeras is modified with 2′-fluoropyrimidines and the shorter RNA strand is unmodified. An exception is the stem loop chimera, which is fully modified. The truncated version of the first-generation chimera (A10-Plk1)[25] is referred to as the blunt chimera, as the *Plk1* siRNA is a blunted duplex (**Fig. 1**), identical to the siRNA part of the first-generation chimera.

To increase the silencing activity and specificity of the A10-Plk1 chimera, we engineered several chimeras, four of which are described here with various modifications in the siRNA portion. First, a chimera with a 2-nt (UU)-overhang at the 3′ end of the siRNA duplex (OVH chimera) was designed to favor recognition by the RNase enzyme Dicer[6]. Second, a wobble base pair was engineered at the 5′ end of the guide (silencing) strand of the OVH chimera by introducing a mutation (C→U) in the passenger strand (G-U wobble chimera). This modification was intended to increase silencing specificity by favoring loading of the guide strand into the RNA-induced silencing complex (RISC)[7,8,27]. Third, we swapped the passenger and guide (**Fig. 1**) strands of the siRNA duplex (swap chimera). This configuration was intended to accommodate 5′ terminal modifications of the shorter RNA strand without loss of function[28,29]. This modification also takes advantage of strand-loading bias introduced by the interaction of the 3′ overhang with the PAZ domains of Argonaute2 (Ago2) and/or Dicer. This configuration favors loading of the guide strand (strand containing 3′ overhang) into RISC[30,31]. Fourth, a stem loop chimera, where the siRNA duplex (stem) is continuous with the aptamer (loop), was designed to mimic endogenous miRNA precursors.

Binding of optimized chimeras to PSMA-expressing cells

We tested the ability of the truncated PSMA aptamer to bind the surface of prostate cancer cells expressing PSMA (cell lines LNCaP and 22Rv1 clone 1.7). A PSMA-negative prostate cancer cell line (PC-3) was used as a control for specificity. Surface expression of PSMA was verified using flow cytometry (data not shown). To determine whether the truncated aptamer can bind the surface of cells expressing PSMA, we incubated ^{32}P-labeled aptamers A10 (ref. 26), A10-3 (57 nt)[26] and A10-3.2 with either LNCaP or PC-3 cells (**Fig. 2a**). Binding of these aptamers was specific for cells expressing PSMA and was dependent on a region within A10-3.2 as this truncated RNA retained specific binding to PSMA-expressing cells. The A10-3.2 aptamer was found to bind LNCaP cells with comparable affinity to the full-length A10 RNA aptamer (**Fig. 2b**).

Next we tested the ability of A10-3.2 to bind to PSMA-expressing cells in the context of the modifications to the siRNA part of the chimeras (**Fig. 2c**). All chimeras retained binding to PSMA-expressing prostate cancer cells. These experiments confirm that modifications made to the first-generation chimera did not affect binding or target specificity.

Effect of chimera modifications on RNAi

To determine whether the second-generation chimeras can silence target gene expression and whether they have enhanced silencing activity compared to the first-generation chimera, we tested for gene-specific silencing using quantitative real time-PCR (qRT-PCR) (**Fig. 3**). PSMA-expressing cells (22Rv1(1.7)) were transfected with increasing amounts (4, 40, 400 nM) of A10-Plk1 or of the second-generation chimeras using a cationic lipid reagent (**Fig. 3a**). As a control, cells were transfected with a control nonsilencing siRNA (Mock). Elevated expression of Plk1 in 22Rv1(1.7) cells was confirmed using immunoblotting (**Supplementary Fig. 1**). This was specific to cancer cells as normal cells (human fibroblasts) have little-to-no Plk1 protein (**Supplementary Fig. 1**). The modifications introduced within the siRNA portion of the chimera, enhanced Plk1 silencing. The most

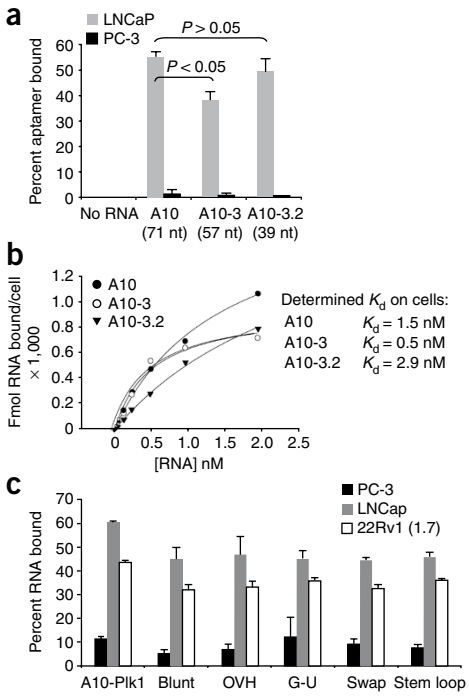

Figure 2 Binding of truncated versions of PSMA A10 aptamer and optimized chimeras to cells expressing PSMA. RNAs were end-labeled with ^{32}P. (**a**) LNCaP cells and PC-3 cells were incubated with either the full-length PSMA aptamer A10 (71 nt) or truncated versions of the PSMA aptamer, A10-3 (57 nt) or A10-3.2 (39 nt). ^{32}P-labeled bound/internalized RNAs were determined by liquid scintillation counter (LSC) or filter binding assay (data not shown). (**b**) Relative affinity of A10 PSMA aptamer and truncated A10 aptamers to cells expressing PSMA. Varying amounts (0–2 nM) of end-labeled A10, A10-3 and A10-3.2 were incubated with fixed LNCaP cells. Bound counts were determined by filter binding assay. (**c**) First-generation chimera (A10-Plk1) and optimized chimeras were incubated with either PC-3 cells (black bars) or LNCaP and 22Rv1(1.7). Cells were processed as in **a**. Bound counts were determined with LSC.

active of the second-generation chimeras were the swap and the stem loop chimeras, which resulted in >99% silencing at concentrations as low as 4 nM.

Next we verified the ability of the second-generation chimeras to silence target gene expression in the absence of transfection reagent (**Fig. 3b**). 22Rv1(1.7) cells were incubated with media containing the various RNA chimeras for 4 d. The modifications made to the siRNA portion of the chimeras substantially enhanced the chimeras' silencing potential (<10% versus >60% for A10-Plk1 and second-generation chimeras, respectively, at 4 nM concentration of the RNAs,) without affecting binding to PSMA on the cell surface. No effect was observed on PSMA-negative prostate cancer cells (data not shown). These experiments indicate that the second-generation chimeras have silencing activities >50 times stronger than that of the first-generation chimera A10-Plk1.

We next assessed whether Dicer can process the siRNA portion of the chimeras in the context of the A10-3.2 PSMA aptamer (**Fig. 4a**). ^{32}P-labeled chimeras (labeled on the 5′-terminus of the short RNA strand) were incubated with recombinant human Dicer for 1 h and 2 h and the cleavage products were analyzed by nondenaturing gel electrophoresis. Incubation with Dicer resulted in ^{32}P-labeled cleaved products corresponding to the size of the duplex Plk1 siRNA (21 mer). These data suggest that the RNA chimeras are Dicer substrates. The size of the ^{32}P-labeled cleaved products (~21 mer) also indicates from which side Dicer enters the chimera and cleaves[32]. These results suggest that Dicer enters from the 3′-end of the longer RNA strand and cleaves ~21 nt upstream. Increased levels of processed duplex in the second-generation constructs compared to the first-generation A10-Plk1 chimera suggest these may be better substrates for Dicer.

Next we tested whether modifications made to the siRNA portion of the second-generation chimeras affect loading of the correct siRNA-silencing strand into RISC (**Fig. 4b**). Loading of the correct strand into the RNAi machinery generates siRNAs with increased activity and reduced off-target effects[10,31,33]. Loading into RISC was assessed by small fragment northern (strand-bias assay)[34]. This assay allows a quantitative measure of the guide strand of the siRNA duplex that is incorporated into RISC and thereby protected from nuclease degradation. The strand that is not incorporated into RISC is rapidly degraded. The assay suggests that modifications made to the first-generation chimera substantially enhanced loading of the correct strand into RISC. Although the addition of the 2-nt (UU)-overhang at the 3′ end of the siRNA duplex alone enhanced loading of the correct strand into RISC, incorporation of a wobble base at the 5′ end of the guide strand had no effect. Notably, swapping the passenger strand with the guide strand resulted in a substantial increase in loading of the guide strand into RISC (**Fig. 4b**). An even greater effect on strand loading was observed with the stem loop chimera, which has the same passenger guide configuration as the swap chimera (**Fig. 4b**). Together, these data indicate that the modifications made to the siRNA portion

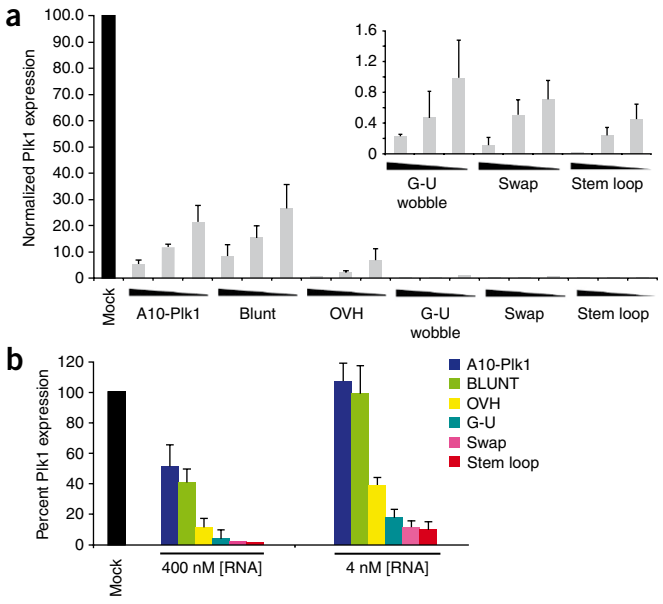

Figure 3 Silencing ability of PSMA chimeras. 22Rv1(1.7) cells were transfected with 400, 40 or 4 nM of each chimera. Cells were processed for qRT-PCR 24–48 h after transfection. Percent Plk1 expression was normalized to that of mock-transfected (mock) cells. (**a**) Comparison of silencing efficiencies of the blunt, OVH, G-U Wobble, swap and stem loop chimeras to that of the first-generation chimera (A10-Plk1). (**a**, inset) Percent Plk1 expression of G-U wobble, swap and stem loop ≤ 1.0 and are depicted on an adjusted *y* axis. Experiments were performed several times (n = 3). (**b**) 22Rv1(1.7) cells were treated with either 400 nM or 4 nM of each of the optimized RNA chimeras in the absence of transfection reagent. Cells were processed for qRT-PCR 4 d after treatments.

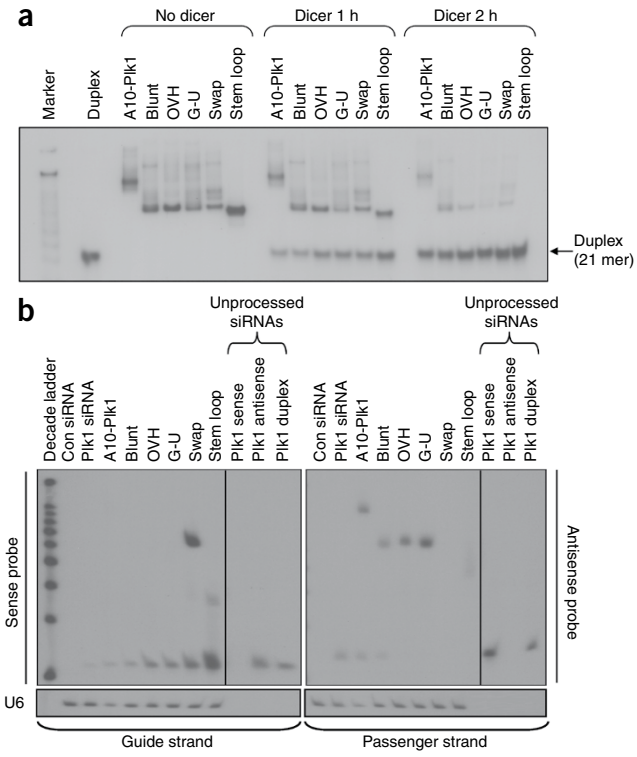

Figure 4 Analysis of chimera processing by the RNAi machinery. (**a**) *In vitro* Dicer processing. The ^{32}P-labeled PSMA-Plk1 chimeras were incubated with recombinant human Dicer enzyme for either 1 or 2 h. The Dicer cleavage or uncleaved (No Dicer) products were visualized after 15% nondenaturing PAGE. (**b**) Assessment of strand bias: loading of siRNA silencing strand into RISC. Small fragment northern blot of RNA isolated from 22Rv1(1.7) cells transfected with 200 pmols of each of the optimized aptamer-siRNA chimera constructs. Loading of the siRNA silencing strand into RISC protects the siRNA strand from degradation (this can be detected with a specific probe using a modified northern blot assay). The strand that is not loaded is rapidly degraded. U6 RNA was used as a loading control. Duplex, Plk1 siRNA duplex; A10-Plk1, first-generation chimera. Blunt, OVH, G-U, swap and stem loop chimeras are described in **Figure 1**. Probe controls show hybridization efficiencies of the sense and antisense probes. The varying intensities of unprocessed chimeras (upper bands on blots) are due to differential probe binding to these species and do not reflect their amounts (this same trend was observed when equal amounts of each chimera was directly loaded on gel and processed as described here (data not shown)).

of the PSMA-Plk1 chimeras enhance silencing activity and specificity by promoting optimal RNAi processing.

Effect of chimeras on prostate cancer cell growth and survival

Depletion of Plk1 in cancer cells leads to a G2/M arrest that decreases cell proliferation and subsequent cancer cell death due to mitotic catastrophe (crisis), a type of cell death which results from mitotic DNA damage[35]. To determine whether treatment with the various PSMA chimeras results in reduced cellular proliferation, 22Rv1(1.7) cells were transfected with each of the chimeric RNAs using a cationic lipid reagent and cell proliferation was measured by ^{3}H-thymidine incorporation (**Fig. 5a**). Mock-treated cells (treated with control nonsilencing siRNA) were used to determine the normal rate of cellular proliferation before treatment. Cisplatin (positive control) was used to inhibit cell proliferation and induce cell death. As previously observed, silencing of *Plk1* by the A10-Plk1 chimera (at 400 nM) substantially inhibited cell proliferation[25]. Lowering the concentration of A10-Plk1 to 4 nM reduced the effect on cellular proliferation by ~sixfold, whereas the second-generation chimeras still inhibited cell proliferation at such low concentrations (**Fig. 5a**). This correlated with cells arrested in the G2/M phase of the cell cycle, as measured by propidium iodide (PI) staining of DNA content and flow cytometry (**Fig. 5b**). Nocodazole, a microtubule-depolymerizing drug, was used as a positive control to arrest cells in G2/M.

Next, we determined whether the second-generation chimeras induced apoptosis in treated cells and whether modifications of the siRNA moiety increased their apoptotic activity. 22Rv1(1.7) cells were treated with 4 nM of the various chimeras in the absence of transfection reagent. Cisplatin was used as a positive control for induction of apoptosis, which was assessed by measuring production of active caspase 3 (Casp3) by flow cytometry (**Table 1** and **Supplementary**

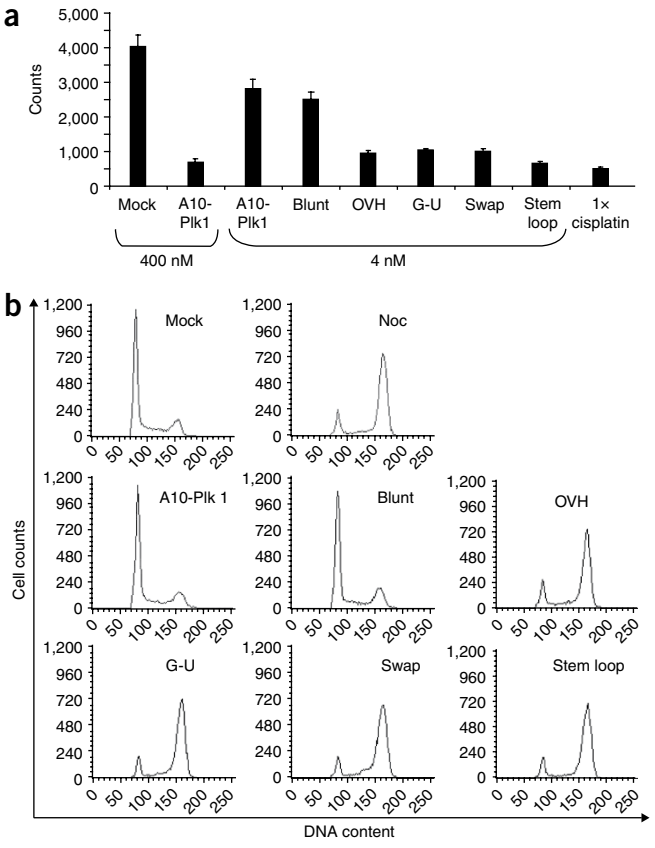

Figure 5 Effect of PSMA-Plk1 chimeras on prostate cancer cell growth. (**a**) 22Rv1(1.7) cells were transfected (or treated in the absence of transfection reagent (data not shown)) with either 400 nM or 4 nM of A10-Plk1 or 4 nM of each of the optimized chimeras. ^{3}H-thymidine was added to the media 24 h after transfection and cells were incubated in the presence of ^{3}H-thymidine for another 24 h. The next day cells were lysed with 0.5 N NaOH and incorporated counts determined by liquid scintillation counter. Cisplatin was used as a positive control for this assay. (**b**) Cell cycle profile of 22Rv1(1.7) cells transfected with 4 nM of each of the optimized chimeras. DNA content of treated cells was determined by flow cytometry 48 h after transfection after staining cells with PI. Nocodazole (Noc) treatment was used as a positive control for this assay to arrest cells in mitosis.

Table 1 Effect of PSMA-Plk1 chimeras on prostate cancer cell viability

Treatment	Concentration	Percent caspase 3 positive cells (average of three experiments)
Untreated	–	17
Cisplatin	2 nM	90
A10-Plk1	400 nM	52
A10-Plk1	4 nM	27
Blunt	4 nM	22
OVH	4 nM	64
G-U	4 nM	72
Swap	4 nM	75
Stem loop	4 nM	85
Plk1 siRNA only	4 nM	13

22Rv1(1.7) PSMA-positive prostate cancer cells were incubated with either 400 nM or 4 nM of A10-Plk1 chimera or 4 nM of each optimized chimera in the absence of transfection reagents. Media containing fresh RNAs was replaced every other day for the course of the experiment. Cells were collected on day 6, stained with an antibody specific for active caspase 3 and processed for flow cytometry. Cisplatin was used as a positive control for apoptosis in this assay. Data were averaged from three independent experiments. (One representative experiment is shown in **Supplementary Fig. 2**).

Fig. 2). As expected, the modifications introduced within the Plk1 siRNA sequence greatly enhanced cell death from 22% (for blunt chimera) to 75 and 85% (for swap and stem loop chimeras, respectively) at a concentration of 4 nM. The swap and stem loop chimeras efficiently induced apoptosis at concentrations 100-fold lower than was necessary for the A10-Plk1 chimera (**Table 1**). Together these data suggest that the modifications made to the second-generation chimeras greatly enhance silencing as well as Plk1-mediated mitotic catastrophe and subsequent cell death.

In vivo efficacy of optimized PSMA-Plk1 chimeras

We next assessed the ability of the second-generation chimeras to limit tumor growth in athymic mice bearing tumors derived from either 22Rv1(1.7) or PC-3 cells (**Fig. 6a**). PSMA expression in tumors was confirmed by immunoblot analysis (**Supplementary Fig. 3a**). For the *in vivo* experiment, we compared the cytotoxic effects of the swap chimera to those of the blunt chimera. Athymic mice (at least ten mice per treatment group) were subcutaneously injected in the flanks with either 22Rv1(1.7) or PC-3 cells. Both cancer cell lines express luciferase[36], which allows measurement of tumor growth using bioluminescence imaging (**Fig. 6a** and **Supplementary Fig. 3b**). Mice with 22RV1(1.7)-derived tumors were injected intraperitoneally each day for a total of 10 d (starting on day 0) with either PBS or 1 nmol each of the indicated chimeric RNAs. Mice bearing PC-3 tumors were treated only with PBS or the swap chimera. No difference in tumor volume was observed in PC-3 tumors after treatment with either PBS or the swap chimera, indicating that the swap chimera did not have nonspecific cell-killing effects (**Fig. 6a**). A pronounced reduction in tumor volume was observed for 22Rv1(1.7) tumors treated with the swap chimera (**Fig. 6a**). In contrast, an increase in tumor volume was observed for tumors treated with PBS or a nonsilencing PSMA chimera, A10-3.2-Con (**Supplementary Fig. 3b**). Notably, ~70% of all swap-treated tumors completely regressed by the end of the treatment. Of the remaining, ~30% (**Fig. 6a**, see inset indicated by arrow for representative tumor-bearing mice), the growth rate of all tumors was slowed by as much as 2.3-fold (**Fig. 6a**). Although regression of PSMA-positive tumors was most evident in swap-treated mice, tumor growth was significantly slowed in mice treated with the blunt chimera (compare PBS with blunt) ($P < 0.001$). No morbidity or mortality was observed following the 10-d treatment with the chimeric RNAs, suggesting that these compounds are not toxic.

As assessed with gross inspection or histological analysis, tumors from mice treated with swap (but not PBS) had liquefactive necrosis–like material that exuded from the tumor mass during gross sectioning. This coincided with large areas of necrosis commonly detected in tumors from the SWAP mice, but substantially less so in those from the PBS-treated mice (**Fig. 6b**). Mitotic cells were detected in all groups including some occasional large and unusual mitotic phenotypes in swap-treated mice. TUNEL staining was seen throughout the tissues as brown staining of random individual cells and along the interface of necrotic and viable tumor tissue. No substantial difference in tumor histology was noted for PC-3 tumors treated with the swap chimera versus the PBS control, suggesting that no nonspecific uptake and subsequent processing of this chimera occurred after systemic administration.

Within each tumor type (22Rv1(1.7) or PC-3), there were no detectable differences in cellular inflammation between treatments (for example, PBS versus swap). Moreover, cellular inflammation was uncommon and mild. Immune cells were detected only along the peripheral border of the tumor and comprised mainly scattered neutrophils with few mononuclear cells. This suggests that tumor regression is not dependent on an immune response. As an additional measure of immune responsiveness, serum from treated mice was screened for levels of interferon-α (INT-α) and interleukin-6 (IL-6) using enzyme-linked immunosorbent assays (ELISA) (**Fig. 6c**). No differences were seen in cytokine levels of mice treated with either PBS or the A10-3.2-Con or swap chimeras. This was in contrast to mice treated with polyinosinic:polycytidylic acid (poly I:C), an established immune stimulator. These data suggest that the chimeras do not trigger an innate immune response and may be safe for *in vivo* applications.

To determine whether the siRNAs released from the chimeras were indeed triggering RNAi *in vivo*, we performed a modified 5′ rapid amplification of cDNA ends (RACE)-PCR (as previously described[25]) on mRNA from tumors of animals treated with the indicated chimeras (**Fig. 6d**). Sequencing of the 5′RACE-PCR products generated with *Plk1*-specific primers demonstrate that Ago2-mediated cleavage occurs between bases 10 and 11 relative to the 5′-end of the guide *Plk1* siRNA strand. PCR products were not observed in samples from control-treated tumors. This result confirms specific siRNA-mediated cleavage products of *Plk1* mRNA in treated tumors *in vivo*.

We next determined whether the addition of a 20 kDa polyethylene glycol (PEG) group could extend the circulating half-life of the swap chimera without affecting binding to PSMA (**Supplementary Fig. 4a**) or Plk1 silencing activity (**Supplementary Fig. 4b**). A 20 kDa PEG was placed at the 5′ end of a *Plk1* siRNA passenger strand by chemical synthesis. This RNA strand included 2′-fluoropyrimidines for decreased nuclease sensitivity. An analogous fully 2′-fluoropyrimidines–modified chimera (swap-2′F) with no terminal PEG was used as a control (**Supplementary Fig. 4b**). First, we verified that the addition of PEG did not abrogate binding specificity and internalization into PSMA-positive prostate cancer cells (**Supplementary Fig. 4a**) and confirmed silencing of *Plk1* mRNA by the PEG-modified chimera (**Supplementary Fig. 4b**).

To determine the *in vivo* half-lives of the swap-2′F and swap-2′F-PEG chimeras, the RNAs were intraperitoneally injected into mice and blood samples were obtained 10 min, 1 h, 5 h and 30 h later. qRT-PCR was used to quantify the amount of RNA present in each blood sample. The *in vivo* circulating half-life of the swap-2′F chimera was substantially increased (from <35 min to >30 h) by the addition of the 20 kDa PEG (**Fig. 6e**, left panel). We next addressed whether the

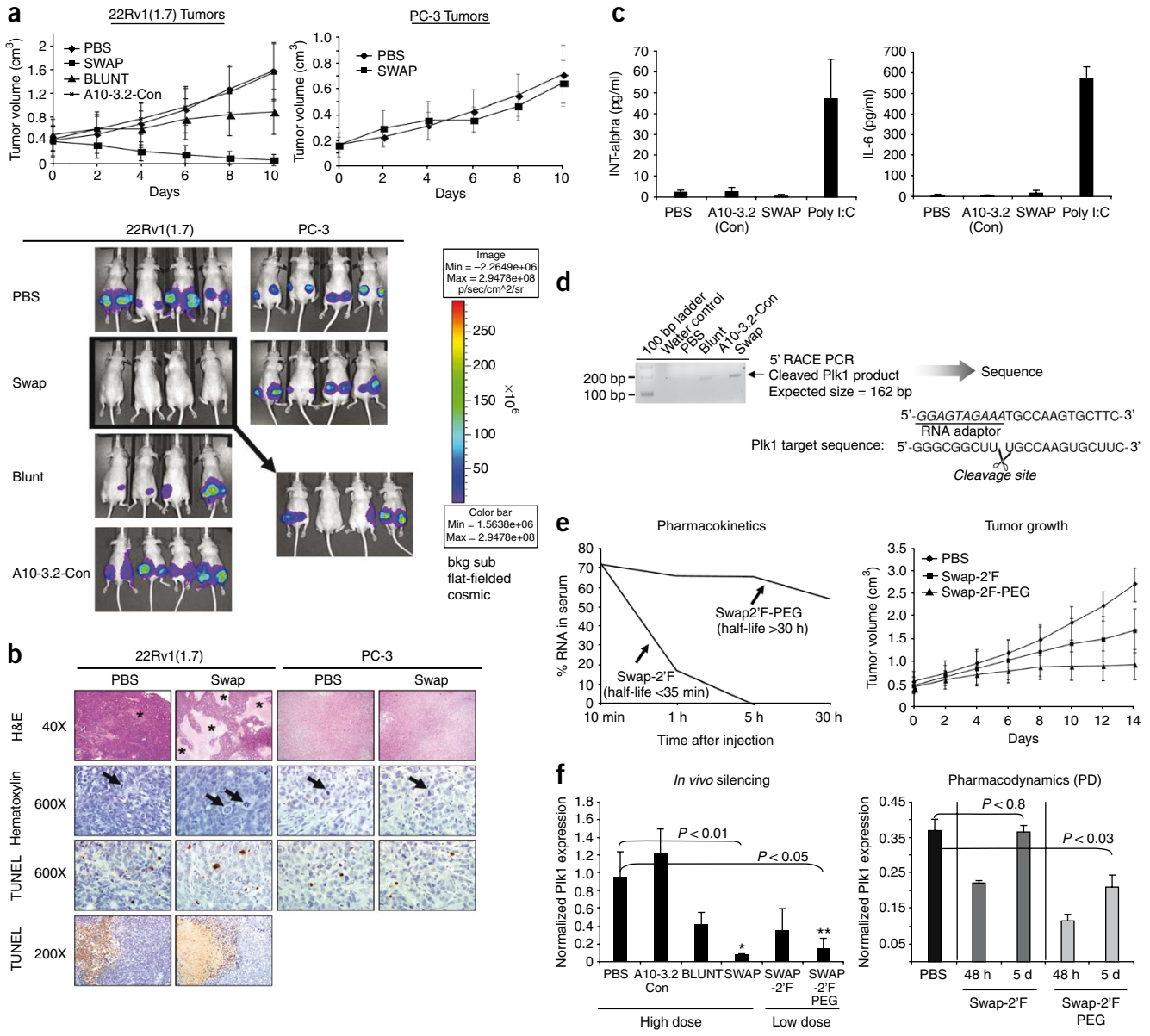

Figure 6 *In vivo* efficacy of optimized PSMA chimera in a xenograft model of prostate cancer. (**a**) 10^6 luciferase-expressing (PSMA-positive or PSMA-negative) prostate cancer cells were injected into the flanks of nude (nu/nu) mice 2 weeks before treatment with optimized chimeras. Treatment with the optimized chimeras commenced when tumors reached a volume of ~0.4 cm^3. 1 nmol of either blunt, swap or A10-3.2-Con was administered intraperitoneally in mice bearing 22Rv1(1.7) tumors. As a control for specificity, a mouse xenograft model of prostate cancer bearing PSMA-negative prostate cancer cells (PC-3) was also treated with the swap chimera. A total of ten treatments were administered for each treatment group. Treatment occurred every day for 10 consecutive days. Tumors were measured with calipers every other day for the course of the experiment. Saline (PBS) treated animals were used as a control. Animals were euthanized 2–3 d after the last treatment. $n \geq 10$ mice per treatment group. Bottom panels: Bioluminescence imaging of 22Rv1(1.7) and PC-3 prostate tumors was carried out after treatment with optimized chimeras (day 10). Examples show tumor growth in four representative animals from each treatment group. Insert indicated by arrow represents bioluminescence imaging images of ~30% of 22Rv1(1.7) tumor–bearing mice treated with the swap chimera that still had palpable tumors (17 out of 48 total tumors) by day 10. All sites represent tumor growth ~25 d after injection of tumor cells. Log-scale heat map (right) of photon flux applies to all panels. (**b**) Histology of 22Rv1(1.7) and PC-3 tumors treated with the various optimized chimeras. Areas of necrosis (asterisks) were readily detected in swap-treated 22Rv1(1.7) tumors, but not frequently seen in PBS-treated tumors (H&E, 40×). Mitotic figures (arrows) were often detected in tumors from all treatment groups including occasional large bizarre mitoses in swap-treated 22Rv1(1.7) tumors (Hematoxylin, 600×). TUNEL staining was detected in scattered cells throughout the tumor section of each group (TUNEL staining, 600×) and at the interface of viable tissue and necrotic foci (TUNEL staining, 200×). Representative sections from the PBS and swap treatment groups are shown. (**c**) Assessment of potential chimera-dependent immunostimulatory effects. Serum from mice treated with either saline (PBS), A10-3.2-Con, swap or poly I:C was screened for levels of cytokines INT-a and IL-6 using ELISA. (**d**) 5′-Rapid amplification of cDNA ends (5′-RACE) PCR analysis to assess siRNA mediated cleavage of Plk1 mRNA in tumors treated with the various PSMA-Plk1 chimeras. (**e**) Pharmacokinetic profile and efficacy of the swap chimera with polyethylene glycol (PEG). (**f**) *In vivo* silencing assessed by quantitative RT-PCR. Plk1 mRNA levels in treated tumors were normalized to GAPDH mRNA levels. Panel on left shows Plk1 levels of tumors (9 tumors/group for this experiment) from animals processed for experiments shown in **a** and **e**.

PEGylation of the swap chimera leads to increased *in vivo* efficacy. Mice bearing 22Rv1(1.7) tumors were intraperitoneally injected with a low dose (250 pmols) of the swap-2′F or swap-2′F-PEG chimeras or with PBS. A total of 5 injections were performed over the course of 10 d. Tumor volume was determined as in **Figure 6a**. The swap-2′F-PEG chimera inhibited tumor growth at substantially lower doses (**Fig. 6a**,**e**, right panel; 10 × 1 nmol versus 5 × 250 pmols). We then determined whether inhibition of tumor growth in treated mice was correlated with silencing of *Plk1* gene expression by the PSMA-Plk1 chimeras (**Fig. 6f**, left panel). *Plk1* mRNA expression was significantly reduced in swap- ($P < 0.01$) and swap-2′F-PEG-treated ($P < 0.05$) tumors compared to PBS control or to A10-3.2-Con.

To determine whether prolonged silencing of *Plk1* gene expression might be responsible for the difference in the *in vivo* efficacies of the swap-2′F-PEG and swap-2′F chimeras (**Fig. 6e**), we carried out a pharmacodynamic study to assess silencing over time (**Fig. 6f**; right panel). In this experiment, PSMA positive tumor–bearing mice were injected with two doses (1 d apart) of 1 nmol each of either swap-2′F or swap-2′F-PEG. Quantitative RT-PCR was then performed on mRNA from tumors to determine the amount of *Plk1* mRNA in the treated tumors at the indicated time points. *Plk1* mRNA silencing is observed in both swap-2′F- and swap-2′F-PEG-treated tumors at 48 h but only in the swap-2′F-PEG-treated tumors 5 d after the last treatment (**Fig. 6f**, right panel). These data indicate that the swap-2′F-PEG chimera has greater gene silencing activity *in vivo*.

DISCUSSION

We developed and characterized PSMA-Plk1 aptamer-siRNA chimeras with enhanced activity, specificity and *in vivo* kinetics relative to the first-generation PSMA-Plk1 chimera[25]. These RNA-only chimeras were optimized by incorporating modifications shown to enhance silencing activity and specificity of siRNA[6–8,27,30,31,33]. The modifications applied to the first-generation chimera include the addition of 2 nt 3′-overhangs and optimization of the thermodynamic profile and structure of the duplex to favor RISC processing of the correct siRNA guide strand[6–8,27,30,31]. Our targeted approach for treating prostate cancer is effective when delivered systemically and is amenable to chemical synthesis for large-scale production.

As many potential therapeutic applications of chimeras, including cancer therapy, require systemic administration of the therapeutic reagent, it is also necessary to optimize the *in vivo* kinetics of these chimeras, in addition to enhancing their potency and specificity. Terminal modification of RNAs with PEG increases the half-life and bioavailability of many oligonucleotide-based therapies, including RNA aptamers[28,37,38]. We found that addition of a 20 kDa PEG to the 5′-terminus of the smaller RNA strand promotes increased retention of the chimera in serum (**Fig. 6e**) without affecting chimera targeting and silencing (**Supplementary Fig. 4**). The PEGylated reagent leads to prolonged-silencing *in vivo* (**Fig. 6f**, right panel) and to inhibition of tumor growth, at lower doses, in mice bearing PSMA-positive prostate tumors (**Fig. 6e**, right panel). Although it is possible that the greater degree of silencing induced by the PEGylated chimera at the 5-d time point is a result of prolonged exposure of the tumor to this reagent, an alternative possibility is that this difference is due to the lingering effects of a greater initial knockdown.

As previously described for the first-generation PSMA-Plk1 chimera (A10-Plk1), cellular targeting of the optimized chimeric RNAs was mediated by the interaction of the aptamer portion of the chimeras with PSMA expressed on the surface of prostate cancer cells (**Fig. 2c**). We found that the first 39 nt of the A10 PSMA aptamer are sufficient for targeting the chimeras to PSMA expressed on the surface of prostate cancer cells. This allowed us to truncate the aptamer portion of the chimeras from 71 nt to 39 nt without loss of function (**Fig. 2**). Chimeras designed with such short aptamers have a long strand of ≤64 bases, a length that can be efficiently produced with chemical synthesis.

Depletion of Plk1 by the 'optimized' chimeras was also specific to PSMA-positive prostate cancer cells (data not shown) and resulted in decreased proliferation and increased apoptosis of the target cells in culture (**Fig. 5a**, **Table 1** and **Supplementary Fig. 2**). Notably, after modifications to the siRNA portion of the chimera, these effects were observed at concentrations of the reagent >50-fold lower than for the 'first-generation' chimera (**Fig. 5a** and **Table 1**). In addition, we found that upon depletion of Plk1, the prostate cancer cells undergo a mitotic arrest (**Fig. 5b**) leading to apoptosis. Coincident with this observation, reducing Plk1 expression has been reported to lead to mitotic catastrophe (crisis) (due to arrest of cancer cells at the G2/M transition of the cell cycle) and death of prostate cancer cells[35]. Notably, this effect is specific to cancer cells; normal cells resume cell-cycle entry upon restoration of Plk1 expression[35,39,40].

An additional measure of specificity was achieved by modifying the siRNA portion of the chimera to enhance loading of the guide strand into RISC (**Fig. 4b**). Optimal loading of the guide strand into RISC is thought to reduce off-target effects that result from inappropriate incorporation of both siRNA strands into the silencing complex[7,8,27,30,31,33]. Although we cannot rule out potential off-target effects mediated by the guide strand itself, these effects would likely be restricted to the tumor, as the siRNAs are targeted to PSMA-expressing prostate cancer cells (**Fig. 6a**).

A major advantage of the PSMA-Plk1 chimera approach as a therapeutic for advanced prostate cancer lies in its target specificity, which is achieved at the level of the aptamer (PSMA-expressing cells are specifically targeted) and at the level of the siRNA (siRNAs are designed against cancer-specific transcripts). Cancer cell-specific targeting could substantially reduce the amount of siRNA needed for effective therapy while reducing systemic cytotoxicity. Most targeted delivery approaches for siRNAs described to date involve the use of complex formulations of synthetic polymers[16–20], proteins[14,15] or charged peptides[12,13]. Although such approaches are proving effective in preclinical studies, their multicomponent formulations complicate production and safety assessment[41]. A one-component system, which involves the direct conjugation of an siRNA to an RNA aptamer, reduces the complexity of the reagent and thus simplifies manufacturing.

2′-fluoropyrimidines in the PSMA-Plk1 chimera increase *in vivo* stability and decrease immunotoxicity, and a terminal 20 kDa PEG increase serum retention. Both modifications are well characterized in humans and are reported to be well tolerated with little toxicity[10,38]. RNA oligonucleotides with similar modifications have already been approved for use in humans (for example, Macugen), with many more quickly moving through the clinical pipeline[10,42–47]. Although we cannot completely rule out potential intracellular toxicity of 2′ fluoropyrimidine–modified RNAs leading to nonspecific immunostimulation[10], based on our findings (**Fig. 6c**) we do not expect these chimeras to produce problematic toxicity in humans.

In principle, the aptamer-siRNA chimera approach can be applied to develop reagents targeting many different cell types provided that a cell-type-specific receptor exists and that an aptamer against the receptor can be selected. The development of an aptamer-siRNA chimera that targets HIV-infected cells supports this notion[32]. The same types of modifications that enabled the *in vivo* efficacy of the PSMA-Plk1 chimera may thus prove useful in developing siRNA-based therapeutics for a wide variety of diseases.

METHODS

Methods and any associated references are available in the online version of the paper at http://www.nature.com/naturebiotechnology/.

Note: Supplementary information is available on the Nature Biotechnology website.

ACKNOWLEDGMENTS

We thank M. Henry (Department of Molecular Physiology and Biophysics, University of Iowa) for supplying PC-3 and 22Rv1(1.7) luciferase-positive cells, A. Klingelhutz (Department of Microbiology, University of Iowa) for providing immortalized human fibroblasts, J. Houtman (Department of Immunology, University of Iowa) for help with flow cytometry, and R. Sousa (Department of Biochemistry, University of Texas Health Science Center) for providing a plasmid encoding a mutant T7 RNA polymerase. We are also thankful to M. Behlke for help with the manuscript. J.P.D. is supported by an National Institutes of Health (NIH) graduate student training grant to the Molecular and Cellular Biology Program (University of Iowa), K.W.T. is supported by a Ladies Auxiliary to the Veterans of Foreign Wars postdoctoral fellowship, J.O.M. and A.P.M. are supported by the NIH. This research was supported by an American Cancer Society Institutional Research Grant and a Lymphoma SPORE Developmental Research Award to P.H.G.

AUTHOR CONTRIBUTIONS

J.P.D., X.-y.L., G.S.T., R.M.W., K.W.T., K.R.S. performed research; D.K.M. provided expertise and analyzed data; A.P.M. provided expertise and useful discussions; J.O.M. designed research, wrote the manuscript and provided useful discussions; P.H.G. designed, coordinated and performed research, analyzed data and wrote the manuscript.

COMPETING INTERESTS STATEMENT

The authors declare competing financial interests: details accompany the full-text HTML version of the paper at http://www.nature.com/naturebiotechnology/.

Published online at http://www.nature.com/naturebiotechnology/.
Reprints and permissions information is available online at http://npg.nature.com/reprintsandpermissions/.

1. Mendenhall, W.M., Henderson, R.H. & Mendenhall, N.P. Definitive radiotherapy for prostate cancer. *Am. J. Clin. Oncol.* **31**, 496–503 (2008).
2. Potvin, K. & Winquist, E. Hormone-refractory prostate cancer: a primer for the primary care physician. *Can. J. Urol.* **15** Suppl 1, 14–20 (2008).
3. Bumcrot, D., Manoharan, M., Koteliansky, V. & Sah, D.W. RNAi therapeutics: a potential new class of pharmaceutical drugs. *Nat. Chem. Biol.* **2**, 711–719 (2006).
4. Aagaard, L. & Rossi, J.J. RNAi therapeutics: principles, prospects and challenges. *Adv. Drug Deliv. Rev.* **59**, 75–86 (2007).
5. de Fougerolles, A., Vornlocher, H.P., Maraganore, J. & Lieberman, J. Interfering with disease: a progress report on siRNA-based therapeutics. *Nat. Rev. Drug Discov.* **6**, 443–453 (2007).
6. Ma, J.B., Ye, K. & Patel, D.J. Structural basis for overhang-specific small interfering RNA recognition by the PAZ domain. *Nature* **429**, 318–322 (2004).
7. Schwarz, D.S. *et al.* Asymmetry in the assembly of the RNAi enzyme complex. *Cell* **115**, 199–208 (2003).
8. Khvorova, A., Reynolds, A. & Jayasena, S.D. Functional siRNAs and miRNAs exhibit strand bias. *Cell* **115**, 209–216 (2003).
9. Wolfrum, C. *et al.* Mechanisms and optimization of *in vivo* delivery of lipophilic siRNAs. *Nat. Biotechnol.* **25**, 1149–1157 (2007).
10. Behlke, M.A. Chemical modification of siRNAs for *in vivo* use. *Oligonucleotides* **18**, 305–319 (2008).
11. Blow, N. Small RNAs: delivering the future. *Nature* **450**, 1117–1120 (2007).
12. Kumar, P. *et al.* Transvascular delivery of small interfering RNA to the central nervous system. *Nature* **448**, 39–43 (2007).
13. Meade, B.R. & Dowdy, S.F. Exogenous siRNA delivery using peptide transduction domains/cell penetrating peptides. *Adv. Drug Deliv. Rev.* **59**, 134–140 (2007).
14. Song, E. *et al.* Antibody mediated *in vivo* delivery of small interfering RNAs via cell-surface receptors. *Nat. Biotechnol.* **23**, 709–717 (2005).
15. Peer, D., Zhu, P., Carman, C.V., Lieberman, J. & Shimaoka, M. Selective gene silencing in activated leukocytes by targeting siRNAs to the integrin lymphocyte function-associated antigen-1. *Proc. Natl. Acad. Sci. USA* **104**, 4095–4100 (2007).
16. Rozema, D.B. *et al.* Dynamic PolyConjugates for targeted *in vivo* delivery of siRNA to hepatocytes. *Proc. Natl. Acad. Sci. USA* **104**, 12982–12987 (2007).
17. Hu-Lieskovan, S., Heidel, J.D., Bartlett, D.W., Davis, M.E. & Triche, T.J. Sequence-specific knockdown of EWS-FLI1 by targeted, nonviral delivery of small interfering RNA inhibits tumor growth in a murine model of metastatic Ewing's sarcoma. *Cancer Res.* **65**, 8984–8992 (2005).
18. Heidel, J.D. *et al.* Administration in non-human primates of escalating intravenous doses of targeted nanoparticles containing ribonucleotide reductase subunit M2 siRNA. *Proc. Natl. Acad. Sci. USA* **104**, 5715–5721 (2007).
19. Howard, K.A. *et al.* RNA interference *in vitro* and *in vivo* using a novel chitosan/siRNA nanoparticle system. *Mol. Ther.* **14**, 476–484 (2006).
20. Pillé, J.Y. *et al.* Intravenous delivery of anti-RhoA small interfering RNA loaded in nanoparticles of chitosan in mice: safety and efficacy in xenografted aggressive breast cancer. *Hum. Gene Ther.* **17**, 1019–1026 (2006).
21. Reich, S.J. *et al.* Small interfering RNA (siRNA) targeting VEGF effectively inhibits ocular neovascularization in a mouse model. *Mol. Vis.* **9**, 210–216 (2003).
22. Bitko, V., Musiyenko, A., Shulyayeva, O. & Barik, S. Inhibition of respiratory viruses by nasally administered siRNA. *Nat Med.* **11**, 50–55 (2005).
23. Li, B.J. *et al.* Using siRNA in prophylactic and therapeutic regimens against SARS coronavirus in Rhesus macaque. *Nat. Med.* **11**, 944–951 (2005).
24. DeVincenzo, J. *et al.* Evaluation of the safety, tolerability and pharmacokinetics of ALN-RSV01, a novel RNAi antiviral therapeutic directed against respiratory syncytial virus (RSV). *Antiviral Res.* **77**, 225–231 (2008).
25. McNamara, J.O. II *et al.* Cell type-specific delivery of siRNAs with aptamer-siRNA chimeras. *Nat. Biotechnol.* **24**, 1005–1015 (2006).
26. Lupold, S.E., Hicke, B.J., Lin, Y. & Coffey, D.S. Identification and characterization of nuclease-stabilized RNA molecules that bind human prostate cancer cells via the prostate-specific membrane antigen. *Cancer Res.* **62**, 4029–4033 (2002).
27. Keck, K. *et al.* Rational design leads to more potent RNA interference against hepatitis B virus: factors effecting silencing efficiency. *Mol. Ther.* **17**, 538–547 (2009).
28. Czauderna, F. *et al.* Structural variations and stabilizing modifications of synthetic siRNAs in mammalian cells. *Nucleic Acids Res.* **31**, 2705–2716 (2003).
29. Boomer, R.M. *et al.* Conjugation to polyethylene glycol polymer promotes aptamer biodistribution to healthy and inflamed tissues. *Oligonucleotides* **15**, 183–195 (2005).
30. Rose, S.D. *et al.* Functional polarity is introduced by Dicer processing of short substrate RNAs. *Nucleic Acids Res.* **33**, 4140–4156 (2005).
31. Sano, M. *et al.* Effect of asymmetric terminal structures of short RNA duplexes on the RNA interference activity and strand selection. *Nucleic Acids Res.* **36**, 5812–5821 (2008).
32. Zhou, J., Li, H., Li, S., Zaia, J. & Rossi, J.J. Novel dual inhibitory function aptamer-siRNA delivery system for HIV-1 therapy. *Mol. Ther.* **16**, 1481–1489 (2008).
33. Reynolds, A. *et al.* Rational siRNA design for RNA interference. *Nat. Biotechnol.* **22**, 326–330 (2004).
34. Pall, G.S. & Hamilton, A.J. Improved northern blot method for enhanced detection of small RNA. *Nat. Protocols* **3**, 1077–1084 (2008).
35. Reagan-Shaw, S. & Ahmad, N. Silencing of polo-like kinase (Plk) 1 via siRNA causes induction of apoptosis and impairment of mitosis machinery in human prostate cancer cells: implications for the treatment of prostate cancer. *FASEB J.* **19**, 611–613 (2005).
36. Drake, J.M., Gabriel, C.L. & Henry, M.D. Assessing tumor growth and distribution in a model of prostate cancer metastasis using bioluminescence imaging. *Clin. Exp. Metastasis* **22**, 674–684 (2005).
37. Bozza, M., Sheardy, R.D., Dilone, E., Scypinski, S. & Galazka, M. Characterization of the secondary structure and stability of an RNA aptamer that binds vascular endothelial growth factor. *Biochemistry* **45**, 7639–7643 (2006).
38. Veronese, F.M. & Mero, A. The impact of PEGylation on biological therapies. *BioDrugs* **22**, 315–329 (2008).
39. Reagan-Shaw, S. & Ahmad, N. Polo-like kinase (Plk) 1 as a target for prostate cancer management. *IUBMB Life* **57**, 677–682 (2005).
40. Strebhardt, K. & Ullrich, A. Targeting polo-like kinase 1 for cancer therapy. *Nat. Rev. Cancer* **6**, 321–330 (2006).
41. Judge, A. & MacLachlan, I. Overcoming the innate immune response to small interfering RNA. *Hum. Gene Ther.* **19**, 111–124 (2008).
42. Dyke, C.K. *et al.* First-in-human experience of an antidote-controlled anticoagulant using RNA aptamer technology: a phase 1a pharmacodynamic evaluation of a drug-antidote pair for the controlled regulation of factor IXa activity. *Circulation* **114**, 2490–2497 (2006).
43. Chan, M.Y. *et al.* Phase 1b randomized study of antidote-controlled modulation of factor IXa activity in patients with stable coronary artery disease. *Circulation* **117**, 2865–2874 (2008).
44. Katz, B. & Goldbaum, M. Macugen (pegaptanib sodium), a novel ocular therapeutic that targets vascular endothelial growth factor (VEGF). *Int. Ophthalmol. Clin.* **46**, 141–154 (2006).
45. Gilbert, J.C. *et al.* First-in-human evaluation of anti von Willebrand factor therapeutic aptamer ARC1779 in healthy volunteers. *Circulation* **116**, 2678–2686 (2007).
46. Girvan, A.C. *et al.* AGRO100 inhibits activation of nuclear factor-kappaB (NF kappaB) by forming a complex with NF-kappaB essential modulator (NEMO) and nucleolin. *Mol. Cancer Ther.* **5**, 1790–1799 (2006).
47. Soundararajan, S., Chen, W., Spicer, E.K., Courtenay-Luck, N. & Fernandes, D.J. The nucleolin targeting aptamer AS1411 destabilizes Bcl-2 messenger RNA in human breast cancer cells. *Cancer Res.* **68**, 2358–2365 (2008).

ONLINE METHODS

This project was approved by the Institutional Animal Care and Utilization Committee (IACUC) of the University of Iowa.

Chemicals were purchased from Sigma-Aldrich. Enzymes were obtained from New England BioLabs (NEB). Cell culture products were purchased from GIBCO BRL/Life Technologies (Invitrogen Corp.). Antibodies were purchased from the following manufacturers: Plk1 (Zymed/Invitrogen); Erk1 K-23 (sc-94); PSMA (Biodesign); β-actin (Sigma-Aldrich); HRP-labeled rabbit anti-mouse IgG secondary antibody (Zymed/Invitrogen).

siRNA sequences. Control siRNA target sequence: 5′-AATTCTCCGAA CGTGTCACGT-3′.

Plk1 siRNA target sequence: 5′-AAGGGCGGCTTTGCCAAGTGC-3′.

Aptamer-siRNA chimera sequences. In italics are the 2′ fluoropyrimidine–modified nucleotides. In the G-U chimera the C in the long RNA strand was mutated to a **U** (bold/underline).

A10-Plk1 chimera. A10-Plk1 sense strand (modified with 2′ fluoropyrimidines): 5′-GGGAGGA*C*GA*U*G*C*GGA*U*CAG*CCAUGUUUACGUCACUCCU UGUCAAUCCUCAUCG*G*CAGACGA*C*UCG*CCC*GAAAGGG*C*GG*CUUU*G *CC*AAG*U*G*C*-3′

Plk1 Antisense siRNA (unmodified RNA): 5′-GCACUUGGCAAAGCCG CCCUU-3′

Blunt chimera. Blunt RNA sense strand (modified with 2′ fluoropyrimidines):

5′-GGGAGGA*C*GA*U*G*C*GGA*U*CAG*CCAUGUUUACGUCACUCCU*AAA AGGG*C*GG*CUUUGCC*AAG*U*G*C*-3′

Plk1 antisense siRNA (unmodified RNA): 5′-GCACUUGGCAAAGCCG CCCUU-3′

*OVH chimera.*OVH RNA sense strand: (modified with 2′ fluoropyrimidines)

5′-GGGAGGA*C*GA*U*G*C*GGA*U*CAG*CCAUGUUUACGUCACUCCU*AAA AGGG*C*GG*CUUUGCC*AAG*U*G*CUU*-3′

Plk1 antisense siRNA (unmodified RNA): 5′-GCACUUGGCAAAGCCG CCCUU-3′

G-U chimera's-U RNA sense strand (modified with 2′ fluoropyrimidines):

5′-GGGAGGA*C*GA*U*G*C*GGA*U*CAG*CCAUGUUUACGUCACUCCU*AAA AGGG*C*GG*CUUUGCC*AAG*U*G***U***UU*-3′

Plk1 antisense siRNA: (unmodified RNA) 5′-GCACUUGGCAAAGCCG CCCUU-3′

Swap chimera. Swap RNA sense strand (modified with 2′ fluoropyrimidines): 5′-GGGAGGA*C*GA*U*G*C*GGA*U*CAG*CCAUGUUUACGUCACUCCU* AAAAGCA*CUU*GGCAAAG*CCGCCCUU*-3′

Plk1 sense siRNA (unmodified RNA): 5′-GGGCGGCUUUGCCAAGUG CUU-3′

Swap-2′F chimera. Swap RNA sense strand (modified with 2′ fluoropyrimidines): 5′-GGGAGGA*C*GA*U*G*C*GGA*U*CAG*CCAUGUUUACGUCACUCCU* AAAAGCA*CUU*GGCAAAG*CCGCCCUU*-3′

Plk1 sense siRNA (modified with 2′ fluoropyrimidines): 5′-GGG*C*GG*C UUUGCCAAGUGCUU*-3′

Swap-2′F-PEG chimera. Swap RNA sense strand (modified with 2′ fluoropyrimidines): 5′-GGGAGGA*C*GA*U*G*C*GGA*U*CAG*CCAUGUUUACGUCAC UCCU*AAAAGCA*CUU*GGCAAAG*CCGCCCUU*-3′

Plk1 sense siRNA: (modified with 2′ fluoropyrimidines)

PEG (20 kDa)-5′-GGG*C*GG*CUUUGCC*AAG*U*G*CUU*-3′ (obtained from TriLink Biotechnologies)

Stem loop chimera (fully modified with 2′ fluoropyrimidines): 5′-GGG*C*G G*CUUUGCC*AAG*U*G*CUU*GGGAGGA*C*GA*U*G*C*GGA*U*CAG*CCAUGUUU*A *C*G*UCACUCCU*AAG*C*A*CUU*GGCAAAG*CCGCCCUU*-3′

A10-3.2-Con chimera. A10-3.2-Con RNA sense strand (modified with 2′ fluoropyrimidines): 5′-GGGAGGA*C*GA*U*G*C*GGA*U*CAG*CCAUGUUUAC*G *UCACUCCU*AA*UUCUCC*GAA*C*G*UG*U*C*A*C*G*UUU*-3′

Con siRNA antisense (unmodified RNA): 5′-ACGUGACACGUUC GGAGAAUU-3′

Generating individual chimeras. Double-stranded DNA templates were generated by PCR as described[25]. Briefly, templates and primers for generating the individual chimeras are listed: PSMA template (5′-GGGAGGACGATGCGG ATCAGCCATGTTTACGTCACTCCTTGTCAATCCTCATCGGCAGACGACT CGCCCGA-3′) was used to generate A10-Plk1, blunt, OVH, G-U, swap, and G-U swap chimeras. The 5′ primer (5′pr) was common to all above chimeras (5′pr: 5′-TAATACGACTCACTATAGGGAGGACGATGCGG-3′)

The 3′primers used to generate each individual chimera are listed:

A10-Plk1 (3′pr: 5′-GCACTTGGCAAAGCCGCCCTTTCGGGCGAGTCG TCTG-3′)

Blunt (3′pr: 5′-GCACTTGGCAAAGCCGCCCTTTTAGGAGTGACGTAA AC-3′)

OVH (3′pr: 5′-AAGCACTTGGCAAAGCCGCCCTTTTAGGAGTGACGT AAAC-3′)

G-U (3′pr: 5′-AAACACTTGGCAAAGCCGCCCTTTTAGGAGTGACGTA AAC-3′)

Swap (3′pr: 5′-AAGGGCGGCTTTGCCAAGTGCTTTTAGGAGTGACGT AAAC-3′)

A10-3.2-Con (3′pr: 5′-AAACGTGACACGTTCGGAGAATTAGGAGTGA CGTAAAC-3′)

The stem loop chimera was generated with the stem loop template oligo (SL-oligo) (5′-AAGTGCTTGGGAGGACGATGCGGATCAGCCATGTTTACG TCACTCCT-3′)

SL 5′ primer: 5′-TAATACGACTCACTATAGGGCGGCTTTGCCAAGTGC TTGGGAGGA

SL 3′ primer: 5′-AAGGGCGGCTTTGCCAAGTGCTTAGGAGTGACGTA AAC

DNA templates were purified with Qiagen DNA purification columns and used in *in vitro* transcription reactions as described[25] to make individual RNA aptamers. All RNAs generated by *in vitro* transcription were produced with 2′ fluoro-modified pyrimidines to render the RNAs resistant to nuclease degradation. With the exception of the stem loop chimera, the 2′ fluoro-modified RNAs generated by transcription for all the other chimeras were annealed to the respective chemically synthesized sense or antisense Plk1 siRNA oligos. The RNAs were annealed at a ratio of 1:4 (RNA oligo:siRNA oligo) in a final concentration of the RNA oligo of 1 μM in DPBS including calcium and magnesium. For the annealing step, the RNA/siRNA mixtures were incubated at 65 °C for 10 min and then allowed to cool slowly at 25 °C for 30 min. Excess siRNA oligo was removed based on size exclusion with a 30 kDa cutoff Amicon spin filter (Millipore).

Cell culture. Normal human foreskin fibroblasts cells (obtained from A. Klingelhutz) were maintained in NuAire water-jacketed CO2 incubators at 37 °C and 5% CO_2 (NuAire) in DMEM supplemented with 10% FBS. Prostate cancer cell lines LNCaP (ATCC) were maintained in Ham's F12-K medium supplemented with 10% FBS. PC-3 and 22Rv1(1.7) luciferase-expressing cells (kindly provided by M. Henry) were grown in RPMI 1640 medium (GIBCO) supplemented with 10% FBS (Hyclone), 1 mM nonessential amino acids (GIBCO) and 100 μg/ml G-418.

^{32}P binding assays. PC-3 or LNCaP and 22Rv1(1.7) cell lines were used for these experiments. For the experiment in **Figure 2a**: 50,000 PC-3 or LNCaP cells (500 cells/μl) in DPBS (plus Ca^{+2} and Mg^{+2}) were blocked with 100 μg/ml tRNA and poly I:C for 15 min. Blocked cells were incubated at 37 °C for 30 min with 500,000–1 million c.p.m. of γ-^{32}P end-labeled A10 aptamer or truncated versions of A10 (A10-3; A10-3.2) in block solution. Cells were then washed profusely with DPBS (plus Ca^{+2} and Mg^{+2}) and bound and/or internalized RNA measured by scintillation counter. Percent aptamer bound was calculated based on input counts. This experiment was performed in triplicate. For determining the relative affinity of the PSMA aptamer and truncated PSMA aptamers, LNCaP cells were fixed in 1% formaldehyde in PBS for 20 min at 25 °C. Fixed cells were washed several times after which cells were diluted and blocked as above. Cells were incubated with serial dilutions of γ-^{32}P end-labeled RNAs ranging from 2 nM to 0 nM at 37 °C for 10 min. The amount of bound RNA was determined by filter binding assay as described in McNamara *et al.*[48] For assessing binding efficacy and specificity of the individual optimized PSMA chimeras, PC-3, LNCaP and 22Rv1(1.7) cells were prepped as for the experiment in **Figure 2a**. Cells were then incubated with 500,000 c.p.m. of γ-^{32}P end-labeled chimeras for 30 min at 37 °C. After several washes with DPBS (plus Ca^{+2} and Mg^{+2}), the amount of bound/internalized

RNA was determined by scintillation counter. The percent of RNA bound was calculated based on input counts.

Silencing assay and quantitative PCR. 22Rv1(1.7) cells were transfected with increasing amounts (4, 40 or 400 nM) of the individual optimized chimeras using Superfect (Qiagen) for 6h (**Fig. 3a**). Alternatively, cells were treated with increasing amounts (4, 40 or 400 nM) of the individual optimized chimeras in the absence of transfection reagent (**Fig. 3b**). 24–48 h (**Fig. 3a**) or 4d (**Fig. 3b**) after treatment, cells were processed for total RNA using RNeasy Kit (Qiagen). For the *in vivo* experiments in **Figure 6f**, tumors from mice treated with the various chimeras were excised and processed for total RNA followed by mRNA extraction as recommended by the manufacturer (RNeasy and Oligotext; Qiagen). Gene silencing was assessed by either qRT-PCR. Real-time PCR was performed on mRNA (50 ng) from 22Rv1(1.7) cells or tumors treated with the various siRNAs or chimeras using iScript One-Step RT-PCR Kit with SYBR Green (Bio-Rad) using an Eppendorf Realplex Mastercycler. All reactions were done in a 50 µl volume in triplicate. Primers for human *GAPDH* and *PLK1* are:

GAPDH forward: 5′-TCGCTCTCTGCTCCTCCTGTTC-3′; *GAPDH* reverse: 5′-CGCCCAATACGACCAAATCC-3′; *PLK1* forward: 5′-GACAA GTACGGCCTTGGGTA-3′; *PLK1* reverse: 5′-GTGCCGTCACGCTCTATGTA-3′. PCR parameters were as follows: 50 °C for 30 min, 5 min of *Taq* activation at 95 °C, followed by 45 cycles of PCR at 95 °C × 30s, 57 °C × 30s, 72 °C × 30s. Standard curves were generated with a serially diluted PCR product as template and the relative amount of target gene mRNA was normalized to *GAPDH* mRNA. Specificity was verified by melt curve analysis and agarose gel electrophoresis. Percent Plk1 mRNA expression in treated cells was determined relative to untransfected/untreated control sample, which was set to 100%.

***In vitro* Dicer assay.** The *in vitro* Dicer assays were performed as described previously[25] with minor modifications. Briefly, the Plk1 guide or passenger strands were end-labeled with T4 polynucleotide kinase (NEB) and γ-^{32}P-CTP. The corresponding strands of the various PSMA-Plk1 RNA aptamers were then annealed, with equimolar amounts, of the labeled siRNA strands in DPBS (plus Ca^{+2} and Mg^{+2}) to form the chimeras. The chimeras (100 pmol) were then incubated with 1 U of human recombinant Dicer enzyme at 37 °C for either 1 h or 2 h, following manufacturer's recommendations (Genlantis). Reactions were stopped with stop buffer and electrophoresed in a nondenaturing 15% polyacrylamide gel. The gels were dried and exposed to X-ray film.

Small fragment northern blots. *Transfection.* 22Rv1(1.7) PC cells were transfected with 200 pmols each of either siRNA duplex, A10-Plk1, blunt, OVH, G-U, swap, or stem loop chimeras using Superfect Reagent. After 24 h cells were processed and RNAs extracted using TRIzol extraction. Untreated cells were used as a negative control for this assay.

Probe synthesis. DNA templates complementary to the sense strand and antisense strand of the Plk1 siRNA were obtained from Integrated DNA Technologies.

Antisense probe: 5′GCACTTGGCAAAGCCGCCCTT3′.

Sense probe: 5′GGGCGGCTTTGCCAAGTGCTT3′.

U6 probe (5′-GCAGGGGCCATGCTAATCTTCTCTGTATCG-3′) was used as an internal loading control.

5 pmols of each probe was 5′ terminally modified through addition of [γ-^{32}P] (6,000 ci/mmol; 8.3 pmol) catalyzed by T4 polynucleotide kinase. Reactions were carried out for 30 min at 37 °C. Reactions were cleaned with a G25 spin columns (GE). Labeled probes were quantified by scintillation counter and equal counts were used for probing the northern blot.

Small fragment northern blot. 20 µg of RNA from each sample and 4 µl of Decade Marker System (Ambion) were heated at 95 °C for 5 min and immediately loaded onto a 15% polyacrylamide-8M urea denaturing Tris buffered saline (TBE) gel. Duplicate gels were loaded. The gels were run at 24 Watts for 3 h after which they were transferred onto a Hybond N+ nylon membrane in 1× TBE on ice for 1 h at 20 V using a semi-dry transfer apparatus. The nylon membranes were cross-linked using a Stratalinker. The membranes were pre-hybridized by incubating in Church's buffer containing 1 mg of boiled salmon sperm DNA at 37 °C for 2 h. Following the prehybridization step, the sense or antisense probes were added directly to the prehybridized blots and incubated at 37 °C overnight. The next day blots were washed 1× with 1× SSC/0.1% SDS for 20 min at 37 °C followed by three more washes with 0.5× SSC/0.1% SDS for 20 min at 37 °C. Blots were exposed overnight at −80 °C. Each blot was stripped by boiling in 0.5% SDS and reprobed for U6.

Proliferation (DNA synthesis) assay. PSMA-positive 22Rv1(1.7) cells were trypsinized and seeded in 12-well plates at ~20,000 cells/well. The next day cells were either transfected or treated in the absence of transfection reagents (data not shown) with either 400 nM or 4 nM of the various aptamer-siRNA chimeras for 24 h. Fresh media containing individual PSMA chimeras and ^{3}H-thymidine (1 µCi/ml medium) was then added to cells to monitor DNA synthesis. After 24 h incubation in the presence of media containing ^{3}H-thymidine, cells were washed twice with PBS, washed once with 5% wt/vol trichloroacetic acid (TCA) (VWR), collected in 0.5 ml of 0.5N NaOH (VWR) and placed in scintillation vials for measurement of ^{3}H-thymidine incorporation.

Cell cycle profile (PI staining). 22Rv1(1.7) cells were seeded on 60 mm plates on day 1. On day 2 cells were transfected or treated in the absence of transfection reagents (data not shown) with 4 nM of the various PSMA chimeras. Cells were processed on day 4 and DNA content measured by PI staining. Briefly, cells were trypsinized and washed several times with DPBS. Cells were then resuspended in NIM Buffer (0.5% BSA; 0.1% NP-40 in PBS) supplemented with 0.1 mg/ml RNase A (DNase free) and 5 µg/ml PI. Nocodazole (Noc) was used as a positive control to arrest cells in mitosis (G2/M phase of the cell cycle). Cells were treated with 100 ng/ml of Noc for 16 h before staining with PI. Stained cells were processed by flow cytometry to measure DNA content.

Cell viability assay (caspase 3). 22Rv1(1.7) cells were either transfected (data not shown) or treated in the absence of transfection reagent (**Table 1** and **Supplementary Fig. 2**) with either 400 nM or 4 nM of the various optimized chimeras. Cells were also treated with medium containing 2 nM cisplatin for 30 h as a positive control for apoptosis. Untreated cells were used as a negative control for the assay. Cells were then fixed and stained for active caspase 3 using a phycoerythrin (PE)-conjugated antibody specific to cleaved caspase 3 as specified in manufacturer's protocol (Pharmingen). Flow cytometric analysis was used to quantify percentage PE-positive cells as a measure of apoptosis.

Tumor implantation and monitoring tumor growth. Athymic nude male mice (nu/nu) 6–10 weeks old were obtained from Harlan Sprague Dawley and maintained in a sterile environment according to guidelines established by the US Department of Agriculture and the American Association for Accreditation of Laboratory Animal Care (AAALAC). Athymic mice were inoculated with 1×10^6 (in 100 µl of 50% Matrigel) of either *in vitro* propagated PC-3 or 22Rv1(1.7) cells subcutaneously injected into each flank. Nonnecrotic 22Rv1(1.7) and PC-3 tumors, which exceeded 0.7 cm in diameter (average ~0.4 cm^3 in volume), were randomly divided into four groups or two groups respectively of ≥10 mice per treatment group. Mice bearing 22RV1(1.7) tumors were treated with: group 1, no treatment (DPBS); group 2, treated with blunt (1 nmol/injection × 10); group 3, treated with swap (1 nmol/injection × 10); group 4, treated with A10-3.2-Con (1 nmol/injection × 10). Mice bearing PC-3 tumors were treated with DPBS or swap (1 nmol/injection × 10); chimera only. Compounds were injected intraperitoneally in 100 µl volumes every day for a total of ten injections. Day 0 marks the first day of injection. Tumors were measured (in two dimensions) every other day with calipers. The following formula was used to calculate tumor volume: $V_T = L \times W^2/2$ (W, the shortest dimension; L, the longest dimension). The growth curves are plotted as the mean tumor volume ± s.e.m. The animals were euthanized 2–3 d after the last treatment and the tumors were excised and formalin fixed for immunohistochemistry. Slides of serial sections were stained with hematoxylin and eosin (H&E) and processed for TUNEL using the ApopTag Kit (Millipore) as a measure of apoptosis. For the PSMA-positive tumors treated with PEGylated swap chimera, athymic nude male mice (nu/nu) 6–10 weeks old were injected with 22Rv1(1.7) cells as indicated above. A total of seven mice per treatment group were injected. After ~3 weeks when tumors had reached 0.7 cm in diameter in the longest dimension, mice were divided into 3 groups: group 1 (DPBS), group 2 (250 pmols/injection swap), and group 3 (250 pmols/injection swap-PEG). Compounds were injected intraperitoneally in 100 µl volumes every other day for a total of five injections. Tumors were measured every other day on the day before the compound injection.

doi:10.1038/nbt.1560

Bioluminescence imaging. To examine tumor size after treatment, we injected luciferin intraperitoneally (50 µl of 15 mg/ml luciferin/10 g mouse body weight) using a 26-gauge needle. Following a 5 min incubation, we performed bioluminescence imaging in a Xenogen IVIS100 imaging system (Xenogen) using a 5 s exposure. Mice were imaged in a dorsal (5 min post-luciferin injection) presentation to monitor tumor growth and/or status after treatment. A mouse was euthanatized when it reached clinical endpoints such as >15% body weight loss or tumors of >2 cm in the longest diameter. We measured whole body tumor growth rates as follows. We placed a circular region of interest (ROI) around the tumor sites of each mouse and quantified total flux using Living Image Software v2.50 (Xenogen) with the units of photons/s/cm^2/sr.

ELISA. Athymic nude male mice (nu/nu) ($n = 6$) were injected with 1 nmol of either A10-3.2-Con or swap chimeras in 250 µl of saline (DPBS). As a positive control for immunostimulation, mice were injected with 200 ng of poly I:C in 100 µl saline. Mice injected with saline alone (250 µl) were used as a negative control. 18 h after injection ~300 µl of blood was drawn from each mouse. The blood was allowed to coagulate at 25 °C before centrifuging the blood samples at 17,000*g* for 10 min to remove erythrocytes and collect serum. Levels of the cytokines IL-6 (R&D Systems) and INT-α (PBL Biomedical Laboratories) in the serum of treated mice were determined by ELISA following manufacturer's recommendations.

5′-rapid amplification of cDNA ends (5′-RACE) PCR analysis. mRNA (10 ng) from tumors treated with different chimeras was ligated to a GeneRacer adaptor (Invitrogen) without prior treatment. Ligated RNA was reverse transcribed using a gene-specific primer 1 (GSP1: 5′-GAATCCTACGACGTGCTGGT-3′). To detect cleavage products, PCR was performed using primers complementary to the RNA adaptor (GR5′pr: 5′-CGACTGGAGCACGAGGACACTGA-3′) and gene-specific primer 2 (GSP2: 5′-GCTGCGGTGAATGGATATTT-3′). The amplification products were resolved by agarose gel electrophoresis and visualized by ethidium bromide staining. The identity of the specific PCR products was confirmed by sequencing of the excised bands.

Pharmacokinetics (PK measurements). C57/BL6 mice ($n = 3$ per treatment group) were injected intraperitoneally with either DPBS or 1 nmol of either swap chimera or swap chimera modified with a 20 kDa PEG group (swap-PEG). Approximately 100 µl of blood volume was retrieved from each mouse at 10 min, 1 h, 5 h, 30 h after injection with compound. The RNA chimeras in blood serum samples were extracted with phenol:chloroform and chloroform. Total RNA in samples was digested with RNase A to remove endogenous RNA and recover nuclease-resistant chimeras. Excess RNase A was removed with a subsequent phenol:chloroform extraction and the RNA chimeras were ethanol precipitated for 2 h at –80 °C by addition of 1/10 volume of sodium acetate, 5 µl of linear acrylamide and two volumes of 100% ethanol. RNA chimera pellets were resuspended in 50 µl of TE and 5 µl of the recovered RNA used for quantitative PCR analysis.

Pharmacodynamics. Athymic nude male mice (nu/nu) 6–10 weeks old were inoculated with 1×10^6 (in 100 µl of 50% Matrigel) *in vitro* propagated 22Rv1(1.7) cells subcutaneously injected into each flank. Nonnecrotic 22Rv1(1.7) tumors, which exceeded 0.7 cm in diameter (~0.4 cm^3 in volume), were randomly divided into three groups as follows: group 1, no treatment (DPBS; $n = 4$); group 2, treated with swap-2′F (1 nmol/injection) ($n = 4$); group 3, treated with swap2′F-PEG (1 nmol/injection) ($n = 4$). Mice were injected on day 1 and then again on day 2 with either DPBS, or 1 nmol each of either the swap-2′F or swap-2′F-PEG chimeras. Tumors from these mice were excised on day 3 (48 h) or on day 5 (5 d). The tumors were processed for total RNA followed by mRNA extraction as recommended by the manufacturer (RNeasy and Oligotext). Silencing of Plk1 gene expression was determined by qRT-PCR as described above.

Statistical analysis. Statistical analysis of tumor size data was conducted using a one-way ANOVA. A *P*-value of 0.05 or less was considered to indicate a significant difference. In addition, two-tailed unpaired *t*-tests were conducted to compare each treatment group to every other.

48. McNamara, J.O. *et al.* Multivalent 4-1BB binding aptamers costimulate CD8 T cells and inhibit tumor growth in mice. *J. Clin. Invest.* **118**, 376–386 (2008).